



IJRASET

International Journal For Research in
Applied Science and Engineering Technology



INTERNATIONAL JOURNAL FOR RESEARCH

IN APPLIED SCIENCE & ENGINEERING TECHNOLOGY

Volume: 12 **Issue:** VI **Month of publication:** June 2024

DOI: <https://doi.org/10.22214/ijraset.2024.63256>

www.ijraset.com

Call:  08813907089

E-mail ID: ijraset@gmail.com

Open Loop Predictive Control of Regular and Chaotic Dynamics of Switched Reluctance Motor

Guidkaya Golam¹, Effa Joseph Yves², Kenmoe Fankem Eric Duckler³

Department of Physics, Faculty of Science, The University of Ngaoundéré, P.O. Box 454 Ngaoundere-Cameroon

Abstract: *The strong non-linearity of the magnetic circuit of switched reluctance machine (SRM) and the strong coupling between the parameters of the dynamic model lead to the unpredictable and chaotic behavior for certain values of its control frequency. This phenomenon which is due to the magnetic resonance of the rotor is characterized by a strong oscillation around an equilibrium position at each control pulse and conduct to chaotic dynamics behavior of SRM. In this work, we apply the technique of predictive control to the chaotic behavior of switched reluctance motor dynamics, in order to ensure a fast convergence of the rotor position towards stable equilibrium positions. The particle swarm optimization algorithm (PSO) is used to obtain an optimal value of the gain of the predictive controller used. Numerical simulations performed using the FEMM (for finite element calculation) and Matlab/Simulink software clearly show a good reduction of the rotor oscillations by applying the predictive control for a frequency taken in the periodic operating range of the machine and a total control of chaos for certain frequencies for which the machine exhibits chaotic behavior without controller. This work can be useful for machine engineers since the dynamic instability can be the cause of vibration and noise in the machine. The results obtained could then be useful and help avoid noisy operation of the machine for industrial applications.*

Keywords: *Switched Reluctance Machine (SRM), Finite Element Analysis (FEA), Particle Swarm Optimization Algorithm (PSO), Chaotic Dynamics, Predictive Control*

I. INTRODUCTION

The switched reluctance machine (SRM) has a good open-loop operation capability [1, 2]. The ability to use an open loop SRM then allows performing a command without speed control. This has the effect of reducing the operation cost and increase the reliability. Indeed, the speed of the machine is related to the frequency of the phase voltage supplied. Thus, for an open loop high speed operation of the SRM, we can just increase the control frequency of the phase voltage. However, the interest of increasing the frequency in order to increase rotation speed can lead to the degradation of dynamic performances, questioning the synchronism principle of the machine. These results were obtained in part of our previous work on the description of the chaotic dynamical behavior of a SRM [3].

Although it has good open-loop operation capability, SRM is highly nonlinear and this makes its study very complex [4]. Compared to conventional machines, a major disadvantage of this machine is the strong torque ripple; phenomenon that contributes to acoustic noises and the mechanical vibration of its rotor [5]. In our previous study, we have shown that for some values of the control frequency, the rotor evolves completely unpredictably. This unpredictability has been likened to chaotic behavior of the machine [3]. However, it has been shown in the literature that torque ripples can be minimized by good optimization of the geometrical structure or by an adequate control technique of the machine [6, 7].

The optimization of the geometrical structure of the machine being very complex, it appears interesting to implement a control technique capable to extending the operation of the machine towards the high open loop control frequencies (without speed sensor). To the best of our knowledge, there is no related works on open loop predictive control of the switched reluctance motor with control of chaos. Indeed, many studies in the literature have focused on closed-loop control of switched reluctance motor without chaos control [8, 9, 10], hence the interest of this study.

The literature review is very rich in terms of chaos control techniques in classical chaotic dynamical systems. The first method of controlling chaos was proposed in 1990 and gave birth to the O.G.Y (Ott, Grebogi and Yorke) method [11]. This method applies to discrete-time chaotic systems or discretized chaotic systems. It consists of disturbing the system by periodically adjusting the control parameter so as to maintain the chaotic trajectory in a chosen periodic orbit. The OGY method is able to stabilize a chaotic dynamic on any unstable periodic orbit (UPO) contained in the chaotic attractor, as soon as its trajectory passes near the chosen UPO. The neighborhood must be chosen "small" so that the disturbance caused by the readjustment of the parameter does not modify the topology of the attractor.

This is the main weakness of this method, which, once locked down, can be very time consuming before the control becomes active. The second method is that of Pyragas (1992) or TDF (time delay feedback) which consists of applying a delayed continuous feedback to force the evolution of the system towards a desired dynamic, whenever the system passes in the vicinity of the desired dynamic behavior. This method applies to continuous time chaotic systems. Other chaos control techniques have been used in the literature to control chaos in classical chaotic dynamical systems. Among them, we can mention the predictive control [12, 1], the generalized backstepping method [10], the backstepping method [13] and several other methods [14, 15, 16].

The dynamic model of a SRM is very complex because of its double nonlinearity (taking into account the phenomena of saturation of the magnetic circuit). It is thus important that the chosen model of chaos controller be the simplest and most effective possible. A heavy model would make the study even more complex. It is for this reason that the predictive control method has been chosen because of its efficiency and simplicity of implementation, both theoretical and experimental. However, for this method, the choice of the controller gain is not always optimized while the controller gain is an important parameter allowing the system to evolve into a stable periodic orbit [12].

The present study therefore uses the predictive control method as a chaos control approach in a conventional open-loop 6/2 SRM considering the saturation phenomena of the magnetic circuit. The problem of obtaining optimal controller gain values for all frequencies is solved by using a particle swarm optimization algorithm coupled to the SRM-Controller set. The simulation results clearly show the reduction of rotor oscillations around the equilibrium positions when the machine is controlled at a periodic operating frequency, the reduction of the response time for selected frequencies in the chaotic behavior range of the machine and finally a complete elimination of chaos in the machine.

II. PRESENTATION OF THE SRM

The study model is a double salience consisting of 6 stator teeth and 2 rotor teeth (DSSRM 6/2) whose geometric dimensions are given in Table 1. In order to facilitate the analysis of the electromagnetic parameters of this machine taking into account of the magnetic saturation phenomena, all the calculating steps have been programmed under the Matlab/Simulink software which will also control the FEMM finite element analysis field calculation software.

A cross-sectional view of this machine drawn with the FEMM software is given in Fig. 1a with the identification of the different parts. Fig. 1b shows an example of a mesh made on this machine where we make an enlargement at the air-gap to show the consistency of the mesh, since it is the electromagnetic exchange zone between the rotor and the stator.

Table 1: Dimensions of the 6/2 SRM [17]

Elements	Value
Number of stator poles N_{ds}	6
Number of rotor poles N_{dr}	2
Lamination outer radius (mm)	45
Airgap (mm)	0.4
Rotor outer radius (mm)	20
Rotor yoke inner radius (mm)	15
Pole arc of stator (deg)	25.25
Pole arc of rotor (deg)	30.5
Length of stator lamination (mm)	40
Number of turns per phase (N)	120

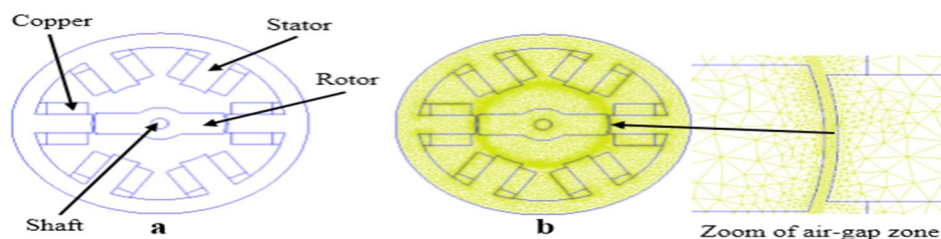


Fig. 1: (a) 2D view of 6/2 SRM, (b) Example of mesh realized

III. MODEL OF 6/2 SRM

The dynamic model of a SRM is given by a system of equations combining the dynamics of phase currents, the rotor position and velocity [3, 18, 19, 20, 21]:

$$\begin{cases} \frac{\partial i_j}{\partial t} = \left(\frac{\partial \psi_j(\theta, i_j)}{\partial i_j} \right)^{-1} \left(U - Ri_j - \frac{\partial \psi_j(\theta, i_j)}{\partial \theta} \frac{\partial \theta}{\partial t} \right) \\ \frac{\partial \Omega}{\partial t} = \left(\frac{1}{J} \right) (T_e - T_L - f_v \Omega) \\ \frac{\partial \theta}{\partial t} = \Omega \end{cases} \quad (1)$$

Where R is the phase resistance, i the current flowing in the phase, U the voltage across a phase of the machine, T_L is the load torque, f_v the viscous friction coefficient, J the moment of inertia, T_e the total electromagnetic torque (sum of the torque produced by the three phases), the expressions $\frac{\partial \psi_j(\theta, i_j)}{\partial i_j}$ and $\frac{\partial \psi_j(\theta, i_j)}{\partial \theta}$ represents the incremental inductance and voltage per speed unity (Back Emf) respectively.

In equation (1), the first row represents the dynamic of the current of j^{th} phase, the second row the dynamic of speed and the third row the dynamic of the rotor position. When taking into account of the phenomenon of saturation of the magnetic circuit, the phase flux is a non-linear function of the current and the position of the rotor $\psi(\theta, i)$. The three phases of the studied SRM being electrically the same, their current dynamics are also the same.

Equation (1) being very complex, the expressions $\frac{\partial \psi_j(\theta, i_j)}{\partial i_j}$ and $\frac{\partial \psi_j(\theta, i_j)}{\partial \theta}$ are obtained from finite element analysis and integrated in the dynamical system of equation (1) [3]. We show on Figure 2 the incremental inductance of one phase as a function of current for some given rotor positions $\psi_l(I, \theta)$ and the Back Emf $\psi_\theta(I, \theta)$ as a function of rotor position for some given phase currents.

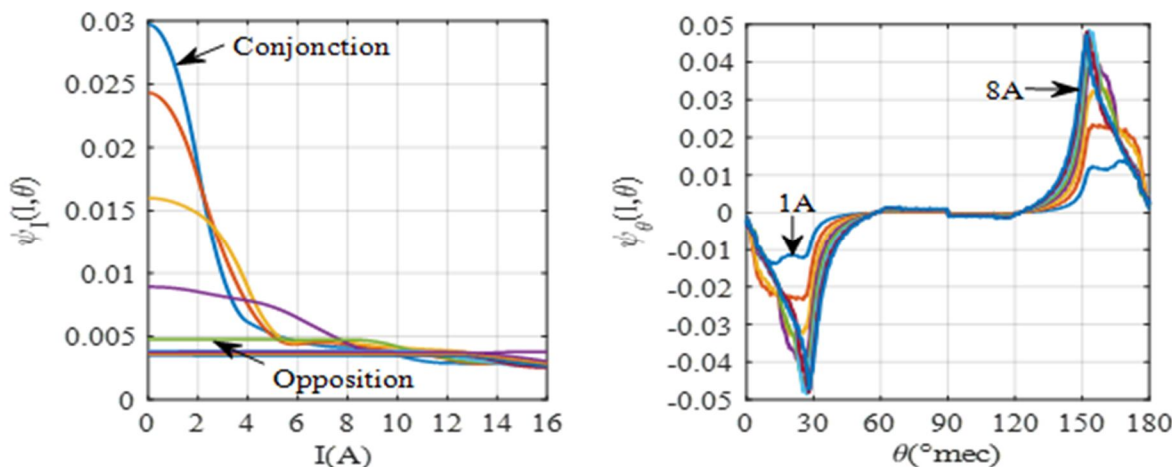


Fig. 2: Incremental inductance $\psi_l(I, \theta)$ and back electromotive force per speed unity $\psi_\theta(I, \theta)$

IV. PREDICTIVE CONTROL METHOD

A. Principle of Predictive Control of Chaos

Consider an n order non-linear chaotic dynamical system which is represented by the following first order differential equation:

$$\dot{x}(t) = f(x(t)) \quad (2)$$

When we add the controller $u(t)$ in system (2), we obtain the following equation (3):

$$\dot{\tilde{x}}(t) = f(\tilde{x}(t)) + u(t) \quad (3)$$

In the case of predictive control, the controller $u(t)$ is considered as the ponderation of the difference between the predicted and the actual state variables. The predicted states can be replaced by the derivation of the systems state variables. Finally, the controller is given by the following equation (4):

$$u(t) = K \left(\dot{x}(t) - \tilde{x}(t) \right) \tag{4}$$

A very complex work is to determine the variable gain K allowing to stabilize the system around unstable periodic orbit or to force the system to pursuit the dynamical behavior needed as the case of the SRM. In order to obtain the optimal gains, we use a stochastic optimization technique: the particle swarm optimization (PSO) method. By using this algorithm, the values of gains will be those obtained at the convergence.

The developed controller will be applied on all phase current dynamics of the studied SRM; the dynamics of speed and rotor position being unchanged. The dynamic of phase current j under control is given by the following relation (equation (5)). Where K

represents the gain of the predictive controller and $\dot{i}_j = \frac{\partial i_j}{\partial t}$ the phase current dynamic without controller (first row of equation (1)).

:

$$\begin{cases} \frac{\partial \tilde{i}_j}{\partial t} = \left(\frac{\partial \psi_j(\theta, \tilde{i}_j)}{\partial \tilde{i}_j} \right)^{-1} \left(U - R\tilde{i}_j - \frac{\partial \psi_j(\theta, \tilde{i}_j)}{\partial \theta} \frac{\partial \theta}{\partial t} \right) + K \left(\dot{i}_j - \tilde{i}_j \right) \\ \frac{\partial \Omega}{\partial t} = \left(\frac{1}{J} \right) (T_e - T_L - f_v \Omega) \\ \frac{\partial \theta}{\partial t} = \Omega \end{cases} \tag{5}$$

In order to obtain the optimal values of the gains of controller, the PSO algorithm is coupled with the controlled system.

B. Optimization of the Gains of Predictive Controller

The optimization of the gains of predictive controller can be done by a deterministic method or a stochastic method (also call metaheuristics method).

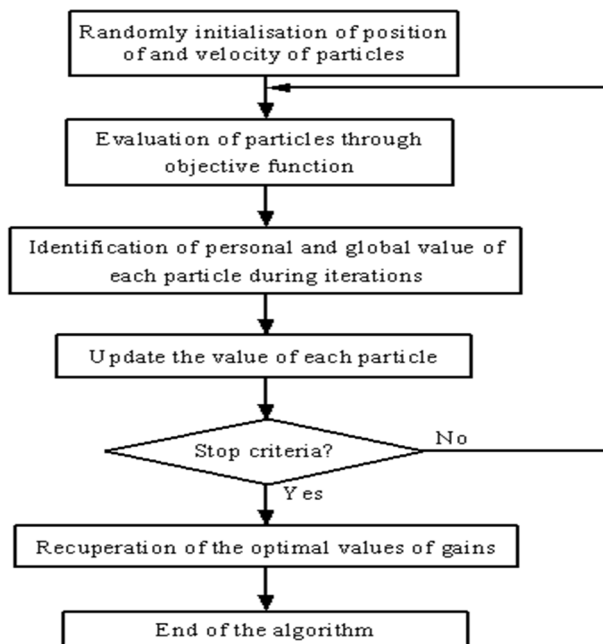


Fig. 3: Flowchart of PSO algorithm

However, the deterministic methods such as sequential quadratic programming, combined gradient and Newton-Raphson, although fast and robust, are adapted only for the objectives functions which present one minimum. Since the objective function has several local minima and a global minimum, the stochastic methods are the most suitable. In the case of our study, we chose the particle swarm optimization algorithm coupled to controller unit of the SRM.

The PSO algorithm belongs to the stochastic methods of evolutionary type with fast convergence proposed by Eberhart and Kennedy (1995). Many applications of this algorithm in several fields, especially in the field of engineering show their superiority compared to other stochastic methods such as the genetic algorithm, biogeography, the ant colony, in terms of robustness and trade-off between speed/accuracy [22]. At each iteration, the values of the particles are updated taking into account the personal best values and the cumulative at the previous iteration. Then the new guides are selected. For its execution, the algorithm steps are gathered in the flowchart presented in Fig.3.

Updating the position and the velocity of each particle is carried out by applying of the following equations (6) and (7) [23]:

$$V_{i+1} = \gamma_1 V_i + \gamma_2 (x_{ip} - x_i) + \gamma_p (x_g - x_i) \tag{6}$$

$$x_{i+1} = x_i + V_{i+1} \tag{7}$$

With γ_1 , the value ranging between 0 and c_1 ; γ_2 and γ_p , the values ranging between 0 and c_2 ; x_{ip} et x_g respectively the best position of a particle i since the first iteration, and the best total position of the swarm. Studies were undertaken in [23] in order to obtain a good convergence starting from the adjustment of the values of c_1 and c_2 . These studies showed that for a better convergence of PSO algorithm, c_1 must be slightly lower than 1 and c_2 must be calculated by the following equation (8).

$$c_1 = \frac{2}{0.97725} c_2 \tag{8}$$

The closer c_1 is to 1, the more exploration of the whole of definition will be better. However, this increases the time of convergence. To reduce this time of convergence, the studies undertaken in [24, 25] introduce a term of inertia. At the beginning c_1 is close to 1 to ensure a complete exploration of the whole of definition. Then, iteration after iteration, c_1 decreases slowly in order to improve the speed of convergence. Thus, the authors define a simple relation (equation (9)) on c_1 , where k is the iteration number:

$$c_1 = \begin{cases} 0.9 - \frac{0.5}{1500 - k} & , \text{if } k < 1500 \\ 0.4 & , \text{if } k \geq 1500 \end{cases} \tag{9}$$

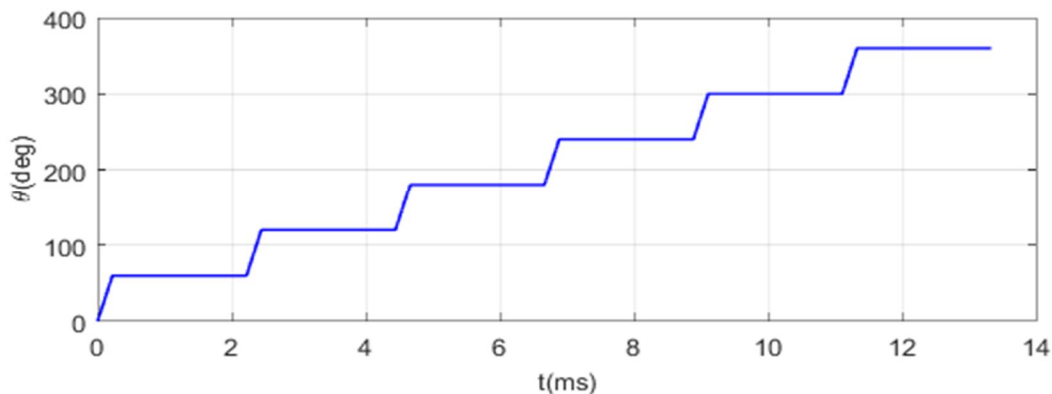


Fig. 4: Example of reference time evolution of rotor position at 150Hz

In the case of the studied machine, the objective function is the minimization of the integral of the absolute error between the generated position of the rotor in an automatic way according to the control frequency for an ideal step by step operation without magnetic phenomenon of resonance and that of the real position of the machine obtained by simulation of the SRM Controller model. This absolute error is given by the following relation:

$$J_{ITAE} = \int_0^{t_{simul}} |e_s| dt \tag{10}$$

Where t_{simul} is the simulation time and e_s the position error. An example of the pace of rotor position generated automatically in the case of an ideal step by step operation at 150Hz is given in Fig.4. This technique will be used for all control frequencies of the studied machine.

V. NUMERICAL SIMULATIONS

A. Chaotic Dynamic of SRM

The bifurcation diagrams presented in the Fig. 5 and Fig. 6 show the evolution of one phase current (since the dynamic ones of the phase current are almost similar) and of the rotor position according to the control frequency. These dynamics come from our previous work [3] where a complete study of the chaotic dynamics of the machine using the tools of chaos theory was made.

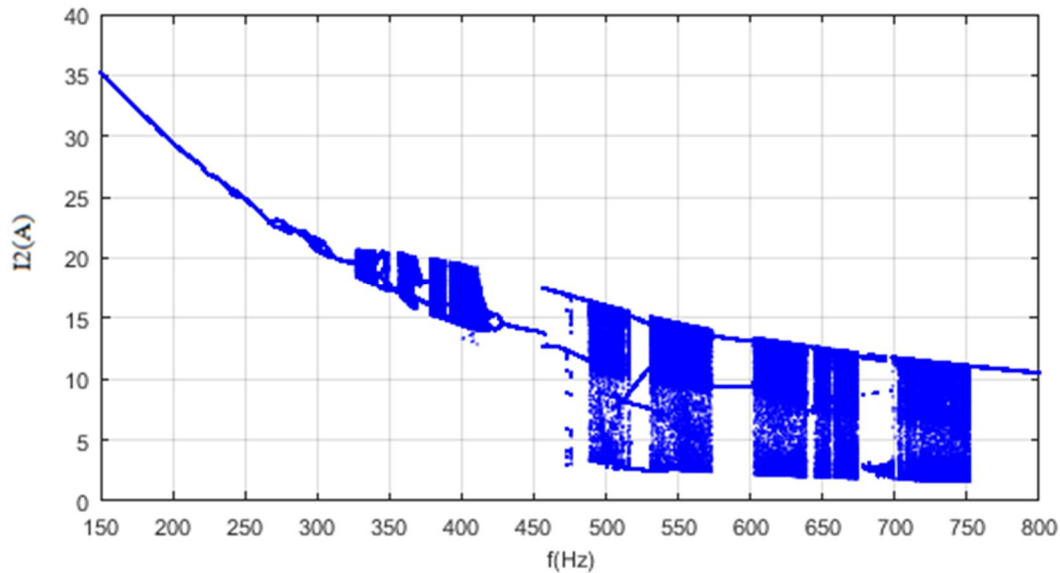


Fig. 5: Bifurcation diagram of current phase 2

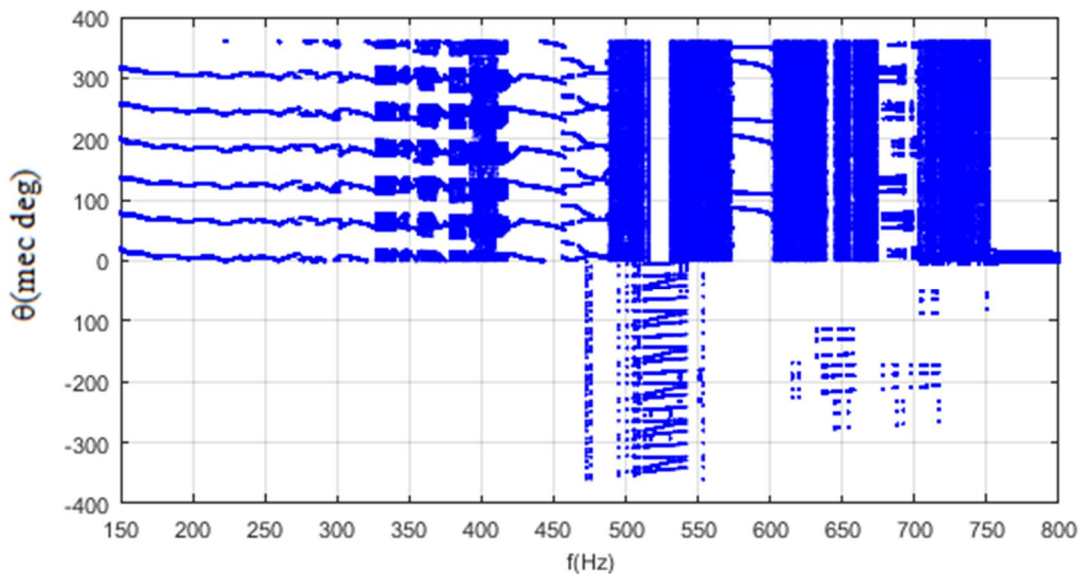


Fig. 6: Bifurcation diagram of rotor position

With an aim of showing the effectiveness of the predictive controller for the reduction of rotor oscillations and the complete elimination of chaos, a study of the time evolution of state variables through the dynamic model is carried out. The frequencies retained for the simulation of the dynamical behavior of the machine without predictive control are summarizing in Table 2.

Table 2: Dynamical behavior of SRM

Frequencies	Dynamical behavior of SRM
150Hz	Period 1 (fundamental)
400Hz	Chaotic: random and unpredictable dynamics of SRM
525Hz	Sub-harmonic of rank 4 : movement in inverse direction
725Hz	Chaotic: random and unpredictable dynamics of SRM

From Table 3, we notice that, for a given control frequency, there exist a value of controller gain able to minimize the error between the ideal rotor position generated at this frequency and the real rotor position of the machine.

Table 3: Optimal gains from PSO

Frequencies	150Hz	400Hz	525Hz	725Hz
K	52.70	70.40	124.30	210.60

The results of numerical simulations confirming this observation are presented in the following sections.

B. Predictive Control at 150Hz

Fig.7 shows the time evolution of the phase current and rotor position, the time evolution of velocity and electromagnetic torque with and without predictive controller for a value of control frequency of 150Hz. The observation of these figures shows a normal dynamic behavior of the machine. At this frequency, the rotor changes stepwise. This behavior is due to the fundamental periodicity of the phase currents. However, around stable equilibrium positions, the oscillations of the rotor are observed in the absence of the controller. This phenomenon that is due to resonance is the first cause of instability in SRM dynamics for high control frequencies. When the predictive controller is active, the oscillations of the rotor are greatly reduced thus causing rapid stabilization of the rotor to the equilibrium positions at each control pulse. The time response of the machine under predictive control is also lower. This phenomenon is clearly visible on the time evolution of the rotor position in Fig. 7d.

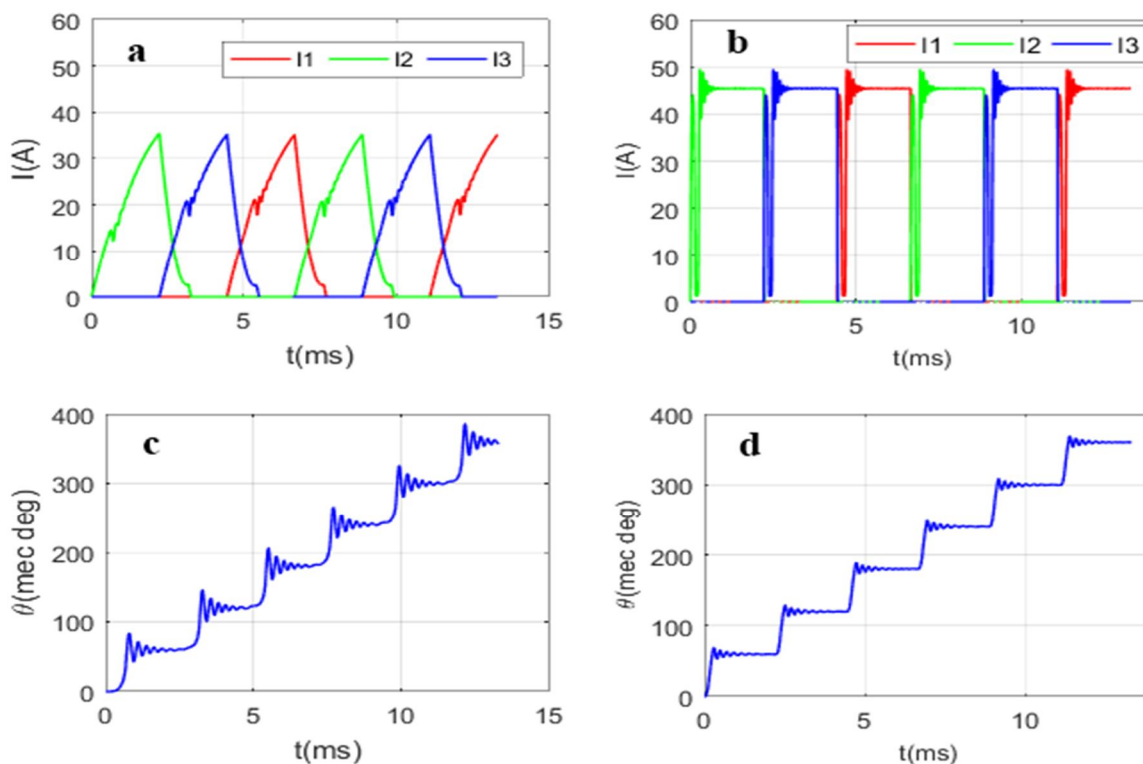


Fig. 7: Time evolution of phase current and rotor position at 150Hz. (a) and (c) without predictive control, (b) and (d) with predictive control

C. Predictive control at 400Hz

At this frequency, it is observed in Fig.8 (a) a disorderly and unpredictable behavior of the machine in the absence of predictive control. The time evolution of the rotor position in the absence of the control (Fig.8 (c)) clearly shows a random behavior of this one with a disordered repetition of losses and step jumps. Because of the strong coupling between the state variables of the dynamic model of SRM, a low instability on one of the state variables has repercussions on all the other variables. The activation of the predictive control forces the system to evolve into a periodic dynamic resulting in a stepwise response of the rotor position (Fig.8d).

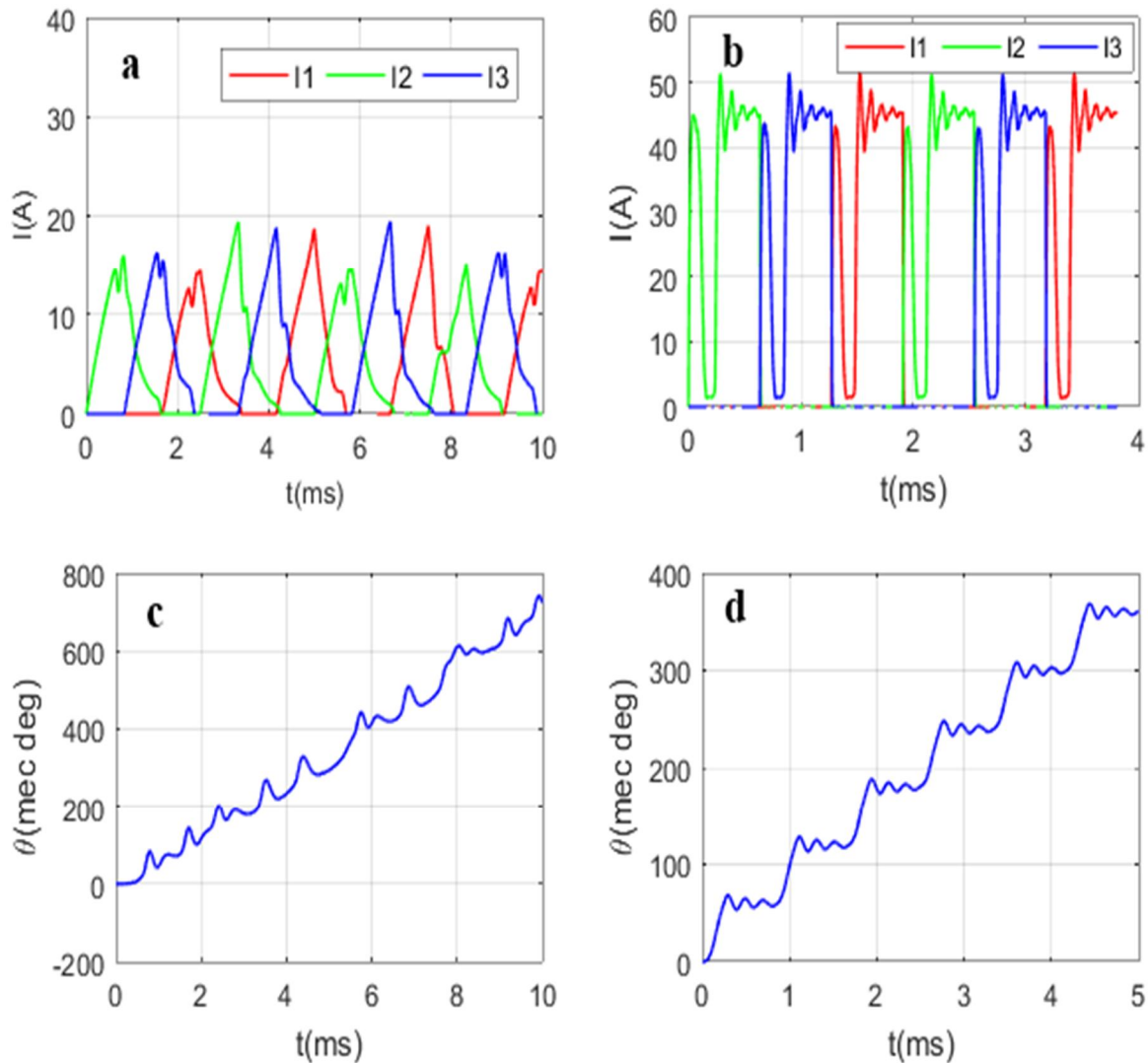


Fig. 8: Time evolution of phase current and rotor position at 400Hz. (a) and (c) without predictive control, (b) and (d) with predictive control

D. Predictive control at 525Hz

This control frequency corresponds to the chaotic dynamic of the machine. At this frequency, the simulation shows the runaway of the machine after a brief transient, in the absence of the predictive controller. Indeed, the observation of the evolution of the rotor position without controller (Fig.9c) shows a change in the rotational direction of SRM. The rotor thus rotates in the opposite direction to the direction previously desired by the control sequence. The control action makes it possible to force the phase currents to follow a fundamental periodic dynamic (Fig.9b), a phenomenon resulting in a stepwise movement of the rotor position (Fig.9d). The predictive controller therefore eliminates the runaway phenomenon of the machine and also leads it towards the direction of rotation imposed by the control sequence used.

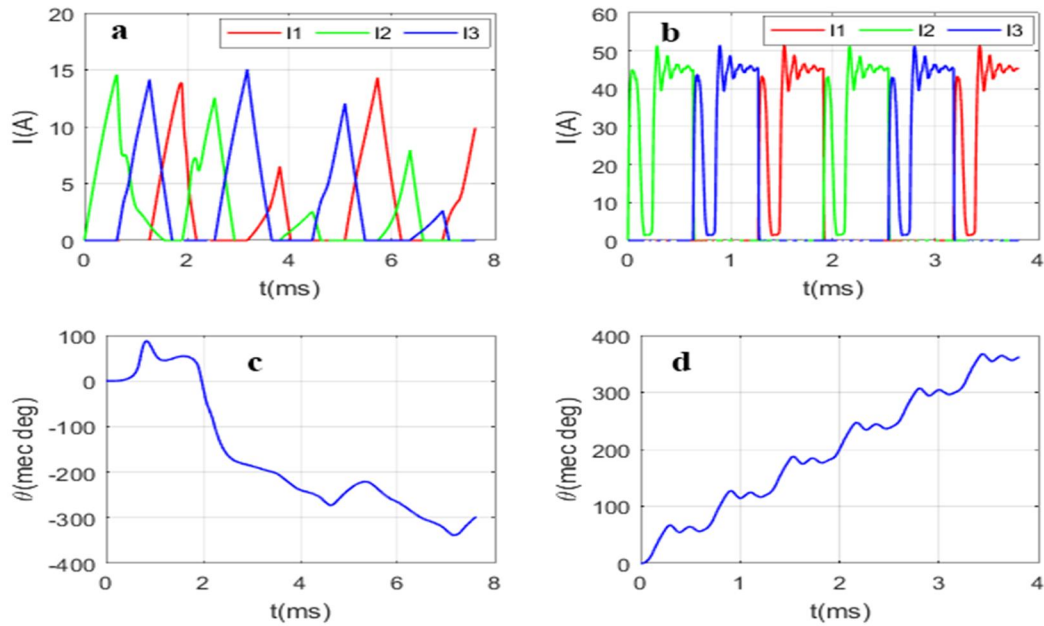


Fig. 9: Time evolution of phase current and rotor position at 525Hz. (a) and (c) without predictive control, (b) and (d) with predictive control

E. Predictive Control at 725Hz

This control frequency also corresponds to the chaotic dynamic of the machine. At this frequency, the rotor rotates in the normal rotational direction imposed by the control sequence, but randomly after a brief change of direction of rotation (Fig.10c) due to the nonuniform dynamics of the departing phase currents from one control period to another in the absence of control (Fig.10a). Fig.10b shows a forcing of phase currents to follow a fundamental periodic dynamic under the action of the predictive controller. There is also a stepwise evolution of the rotor position as a function of time (Fig.10d). As for the previous results, a simple instability on one of the state variables has repercussions on all the characteristic variables of the dynamic model of SRM. The action of the controller thus makes it possible to totally eliminate the chaos in this machine and forces it to follow a periodic behavior. Thus, all the variables of the dynamic model of the machine follow a regular dynamic behavior under the action of the predictive controller as shown in Fig.10.

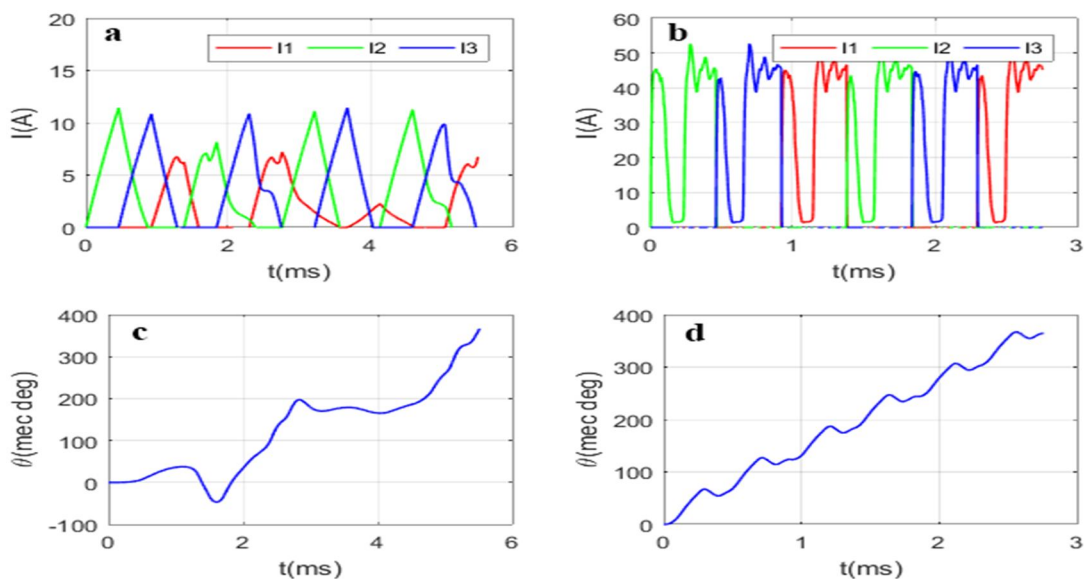


Fig. 10: Time evolution of phase current and rotor position at 725Hz. (a) and (c) without predictive control, (b) and (d) with predictive control

At the control frequencies of 400Hz, 525Hz and 725Hz, the SRM exhibits a chaotic dynamic behavior. In order to further highlight, the multiplicity of periods in the evolution time of phase currents in the absence of predictive controller and the total elimination of chaos after activation of the predictive controller, it is necessary to represent phase portraits. Fig.11 shows the phase portraits in the plane (I_1, I_2) respectively with and without controller, for a control frequency of 725Hz.

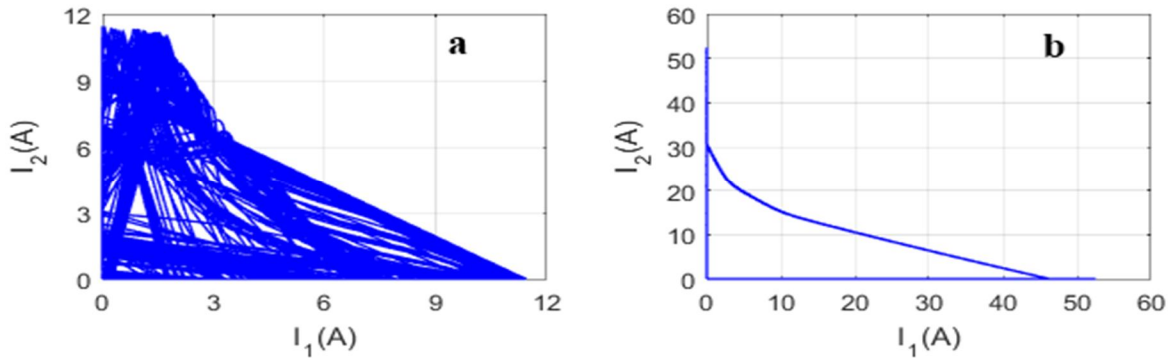


Fig. 11: Phase portrait in the plane (I_1, I_2) at 725Hz. (a) without predictive control, (b) with predictive control.

Observation of Fig.11 clearly shows the passage of a multiplicity of period (chaotic attractor) to a limit cycle of period 1, under the action of the predictive controller. These results therefore confirm the total elimination of chaos in the dynamic behavior of the machine at this control frequency.

VI. ROBUSTNESS TESTS

The results of control previously presented showed the performances of predictive controller in the stabilization of an unstable periodic orbit. However, the parameters of the dynamic model are likely to vary with the temperature, the load torque or with the operation conditions. Thus, the dynamic behavior of the machine can be completely modified. In this section, the performances of the predictive controller are evaluated through the variation of some parameters of the dynamic model such as load torque, phase resistance, moment of inertia, viscous friction coefficient. All the simulations are made for the control frequency of 400Hz which corresponds to a chaotic behavior in the absence of predictive controller.

A. Effect of Variation of load Torque T_L

The load torque is initially null and the predictive controller is activated. At the instant $t = 5\text{ms}$, the load torque passes from 0 to 0.2Nm. The results of dynamic simulation are summarized on Fig.12.

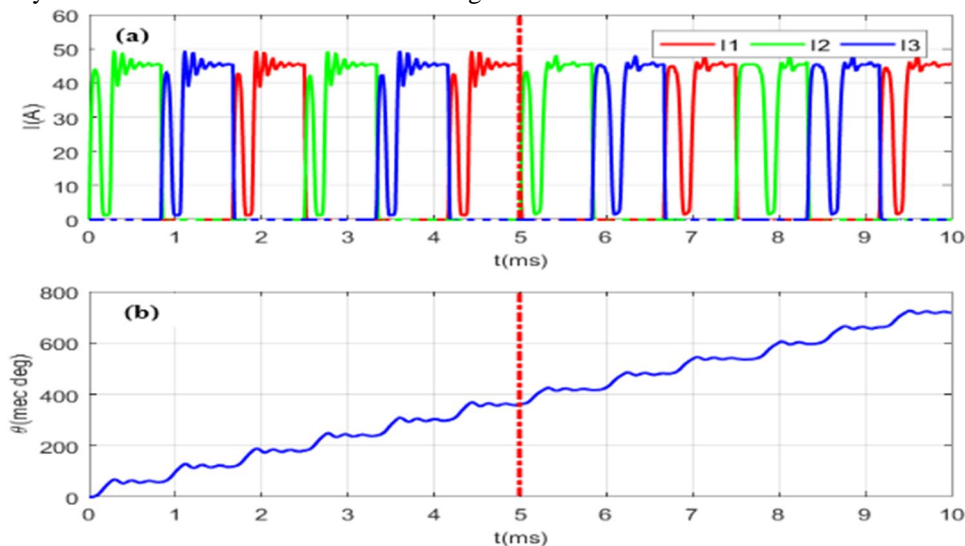


Fig. 12: Dynamics behavior of SRM with variation of load torque when $F = 400\text{Hz}$: (a) currents response, (b) rotor position response

The observation of these figures clearly let conclude that the predictive controller associated with the phase currents dynamics of the machine is robust for the variation of load torque (within the limits of possible). The dynamics basically step by step of the rotor position is the total proof of the rejection of this disturbance. However, a weak influence on the phase currents dynamics is observed.

B. Effect of Variation of Phase Resistance R

The description of this test is made by considering an increase of 25% of the value of phase resistance R at instant $t = 5\text{ms}$. The results of simulations are presented on the Fig.13. We notice through these graphics that the increase of phase resistance involves the reduction of the values of phase currents. The predictive controller thus allowed balancing the total dynamics of the machine. In addition, we notice that this variation of phase resistance does not present impact on the mechanical behavior of the machine, which is clearly visible on the fundamental step by step behavior of the rotor position. Thus, only the electric variables are affected.

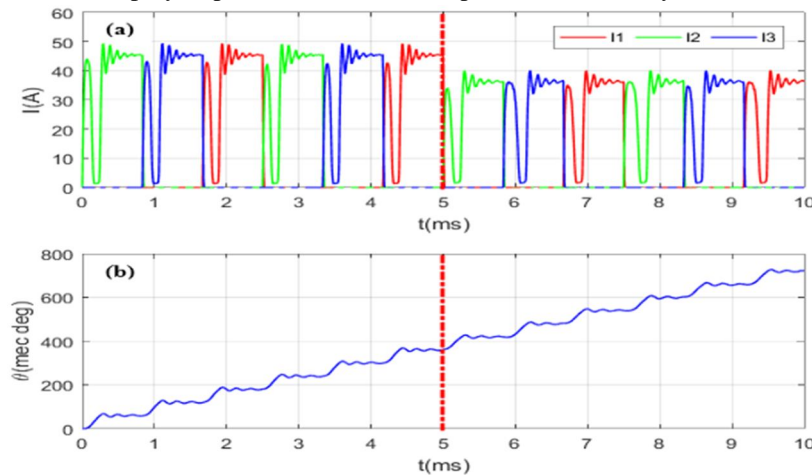


Fig. 13: Dynamics behavior of SRM with variation of phase resistance when $F = 400\text{Hz}$: (a) currents response, (b) rotor position response

C. Effect of variation of moment of inertia J

As in the case of the resistance of the phases, the moment of inertia increases by 25% of its initial value at the moment $t = 5\text{ms}$. The results of simulations are presented on the Fig.14. We also observe here a weak influence of the variation of the moment of inertia on the total mechanical behavior of the machine under predictive control. The dynamic of the machine thus remains in a fundamental periodic behavior. However, this variation of the moment of inertia increases the oscillations of the phase currents dynamic.

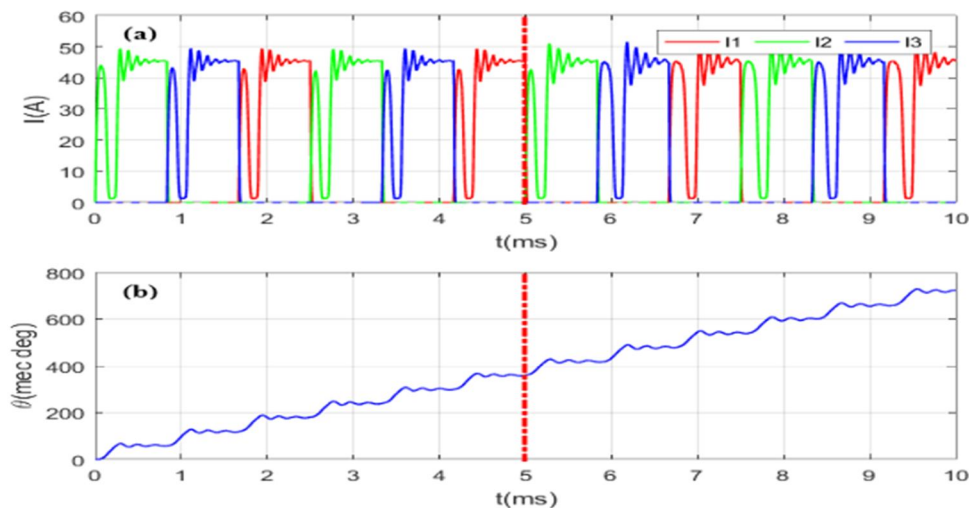


Fig. 14: Dynamics behavior of SRM with variation of the moment of inertia when $F = 400\text{Hz}$: (a) currents response, (b) rotor position response

D. Effect of variation of viscous friction coefficient f_v

The results on Fig.15 show the dynamics of the SRM with an increase of 25% of the viscous friction coefficient on its initial value at the instant $t = 5$ ms. The dynamic evolution of the rotor position remains almost unchanged. However, a reduction of the oscillations is observed on the dynamics of phase currents. One can tell that despite of the parameter mismatch, the proposed predictive control with optimal values of gain remains robust with a total disturbance rejection. In the future work, we plan to validate this observation by an experimental study.

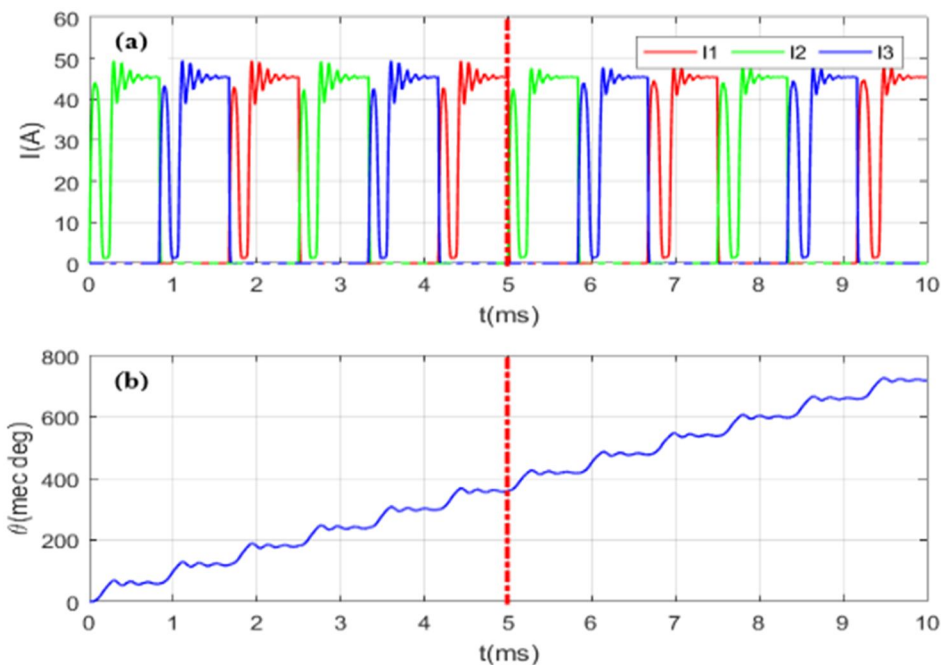


Fig. 15: Dynamics behavior of SRM with variation of viscous friction coefficient when $F = 400$ Hz: (a) currents response, (b) rotor position response

VII. CONCLUSION

In this work, the predictive chaos control technique was used to reduce or eliminate the instabilities and multiplicity of periods appearing in the dynamic behavior of a 6/2 SRM, taking into account of the magnetic saturation phenomenon. The mathematical model of the 6/2 SRM was presented. A rich and varied dynamical behavior including chaos was obtained by plotting the bifurcation diagram of the system. Faced to the difficulty in calculating the gain of the predictive controller in the case of the doubly non-linear dynamic model, a stochastic method using the particle swarm optimization algorithm has been employed to derive optimal gains for some values of the control frequencies. Using these optimal gains, numerical simulations using the Matlab/Simulink software have shown a reduction in rotor oscillations around the equilibrium positions for a control frequency of 150Hz and elimination of chaos for the following control frequencies 400Hz, 525Hz and 725Hz. In addition, the analysis of the robustness has shown good performances of the controller with a total disturbance rejection which can occur spontaneously but also voluntary. In perspective, we plan to carry out a complete study of the machine under predictive control for the entire frequency range presented by the bifurcation diagram. Finally, an extension of the operation of the machine outside the frequency range used in this work will be done.

REFERENCES

[1] Boukabou, A. Chebbah et N. Mansouri, « Predictive control of continuous chaotic systems,» International Journal of Bifurcation and Chaos, n° 118, pp. 587-592, 2008.

[2] G. Zwe-Lee, K.-Y. K, H. Jia-Sheng, H. Min-Fu et T. MingHsiao, Design and Optimization of High-Speed Switched Reluctance Motor Using Soft Magnetic, <https://doi.org/10.1109/IPEC.2014.6869593>, 2014.

[3] G. Guidkaya, J. Y. Effa et F. E. D. Kenmoe, «Chaotic dynamic behavior in switched reluctance motor taking into account magnetic saturation effects,» International Journal of System Assurance Engineering and Management, vol. 13, p. 1556-1571, 2022.

[4] A. Tahour, Meroufel, H. Abid et A. Aissaoui, « Sliding Controller of Switched Reluctance Motor,» Leonardo Electronic Journal of Practices and Technologies, vol. 12, pp. 151-162, 2008.

- [5] V. Prabhu, V. Rajini et M. Balaji, « A Comparative Study of Operating Angle Optimization of Switched Reluctance Motor with Robust Speed Controller using PSO and GA,» J Electr Eng Technol, 2015.
- [6] B. Mirzaeian, M. Moallem, V. Tahani et C. Lucas, «Multiobjective optimization method based on a genetic algorithm for switched reluctance motor design,» IEEE Transactions on Magnetics, vol. 38, pp. 68-75, 2002.
- [7] Z. Xu, R. Zhong, L. Chen et S. Lu, « Analytical method to optimize turn-on angle and turn-on angle for switched reluctance motor drives,» Electric Power Applications, IET , vol. 6, pp. 593-603, 2012.
- [8] I. M. Namazi, A. Rashidi et M. Saghalian-Nejad, «Energy-based adaptative sliding mode speed controlfor switched reluctance motor drive system,» Iranian Journal of Electrical and Electronic Engineering, vol. 8, pp. 68-75, 2012.
- [9] L. Chouaib, S. Kamel, M. Belkacem, M. T. Benchouia et M. E. H. Benbouzid, «Speed control of 8/6 switched reluctance motor with torque ripple reduction taking into account magnetic saturation effects,» Energy Procedia, vol. 74, pp. 112-121, 2015.
- [10] R. Sahab et Z. Haddad, «Chaos control in nonlinear systems using the generalized backstepping method,» American Journal of Engineering and Applied Sciences, vol. 1, pp. 378-383, 2008.
- [11] E. Ott, C. Grebogi et A. Yorke, «Controlling chaos,» Physic. Rev. Lett, vol. 64, pp. 1196-1199, 1990.
- [12] T. Ushio et S. Yamamoto, «Prediction-based control of chaos,» Physics Letters A, 1999.
- [13] G. Chen et X. Dong, «On feedback control of chaotic continuous-time systems,» IEEE trans on CAS, 1993.
- [14] A. Boukabou et N. Mekircha, «Generalized chaos control and synchronization by nonlinear high-order approach,» Mathematics and Computer in Simulation, 2012.
- [15] J. Slotine, «Sliding controller design for nonlinear systems,» International Journal of Control.
- [16] X. Liu, « Impulsive stabilization and control of chaotic system,» Nonlinear Analysis, 2001.
- [17] I. Gourragui, «Modelisation numerique, optimization et commande de Machines à Reluctance Variable,» PhD thesis University of Metz, France, 2006.
- [18] M. R. Harris, A. Hughes et P. J. Lawrenson, «StaticTorque Production in Saturated Doubly-Salient Machines,» Proc. IEE, pp. 1121-1127, 1975.
- [19] R. S. Wallace et D. G. Taylor, «Three Phase Switched Reluctance Motor Design to Reduce Torque Ripple,» International Conference on Electrical Machines ICEM'90, pp. 782-787, 1990.
- [20] J. Reinert, R. Inderka, M. Menne et D. R. W. De, «Optimisation Performance in Switched Reluctance Motor,» In APEC '98 Thirteenth Annual Applied Power Electronics Conference and Exposition, 2000.
- [21] M. Sanada, S. Morimoto, Y. Takeda et N. Matsui, «Novel Rotor Pole Design of Switched Reluctance Motorsto Reduce the Acoustic Noise,» In Conference Record of the 2000 IEEE Industry Applications Conference. Thirty-Fifth IAS Annual Meeting and World Conference on Industrial Applications of Electrical Energy (Cat. No.00CH37129), 2000.
- [22] F. Nzanywayingoma et Y. Yang, «Analysis of Particle Swarm Optimization and Genetic Algorithm based on Task Scheduling in Cloud Computing Environment,» International Journal of Advanced Computer Science and Applications, vol. 8, pp. 19-25, 2017.
- [23] M. Clerc et P. Siarry, «Une nouvelle mta-heuristiquepour l'optimisation difficile : la methode des essais particuliers,» J3EA 3, 007. DOI:10.1051/bib-j3ea:2004007, 2004.
- [24] Y. Shi et R. C. Eberhart, «Empirical study of particle swarm optimization, Evolutionary Computation,» CEC 99, Proceedings of the 1999 Congress on 6-9 July 1999, vol. 3, pp. 1950-1953, 2003.
- [25] C. T. Ioan, « The particle Swarm Optimization algorithm: convergence analysis and parameters selection,» Information Processing Letters, pp. 317-325, 2003.



10.22214/IJRASET



45.98



IMPACT FACTOR:
7.129



IMPACT FACTOR:
7.429



INTERNATIONAL JOURNAL FOR RESEARCH

IN APPLIED SCIENCE & ENGINEERING TECHNOLOGY

Call : 08813907089  (24*7 Support on Whatsapp)